

NACA RM 152G22

NOV-3 1952

UNCLASSIFIED



# RESEARCH MEMORANDUM

## FOR REFERENCE

NOT TO BE TAKEN FROM THIS ROOM

THE EFFECTS OF CAMBER AND LEADING-EDGE-FLAP DEFLECTION  
ON THE PRESSURE PULSATIONS ON THIN RIGID AIRFOILS  
AT TRANSONIC SPEEDS

By Milton D. Humphreys and John D. Kent

Langley Aeronautical Laboratory  
Langley Field, Va.

CLASSIFICATION CANCELLED

NACA R 2755 Date 10/12/54

By M.D.H. 11/9/54 See

CLASSIFIED DOCUMENT

This material contains information affecting the National Defense of the United States within the meaning of the espionage laws, Title 18, U.S.C., Secs. 793 and 794, the transmission or revelation of which in any manner to unauthorized person is prohibited by law.

### NATIONAL ADVISORY COMMITTEE FOR AERONAUTICS

WASHINGTON

October 27, 1952

UNCLASSIFIED

NACA LIBRARY

LANGLEY AERONAUTICAL LABORATORY  
Langley Field, Va.



UNCLASSIFIED

## NATIONAL ADVISORY COMMITTEE FOR AERONAUTICS

## RESEARCH MEMORANDUM

## THE EFFECTS OF CAMBER AND LEADING-EDGE-FLAP DEFLECTION

## ON THE PRESSURE PULSATIONS ON THIN RIGID AIRFOILS

## AT TRANSONIC SPEEDS

By Milton D. Humphreys and John D. Kent

## SUMMARY

The effects of camber and leading-edge-flap deflection on the pressure pulsations on thin rigid airfoils at Mach numbers from 0.5 to 1.0 have been investigated. The tests included variations in camber corresponding to design lift coefficients of 0, 0.2, and 0.5, as well as variations in deflection of a 15-percent-chord leading-edge flap from  $0^\circ$  to  $-15^\circ$  on a 6-percent-thick NACA 64A-series airfoil. The high pulsations associated with leading-edge flow separation on the basic airfoil were significantly reduced either by use of camber or by suitable deflection of a 15-percent-chord leading-edge flap. The optimum camber or flap deflection were dependent on Mach number and normal-force coefficient. Comparison of the data for the basic 64A006 section used in these tests with data previously obtained for the 65A006 section revealed significantly lower pressure pulsations for the 65A006 airfoil.

## INTRODUCTION

An earlier investigation of pressure pulsations on rigid airfoils showed that decreasing the airfoil thickness was beneficial in reducing the magnitude of the pressure pulsations at high subsonic Mach numbers (ref. 1). On the 4- and 6-percent-thick airfoils, at Mach numbers around 0.65, however, high-pressure pulsations were encountered, particularly near the leading edge, as a result of leading-edge flow separation which started to occur at moderate angles of attack. The leading-edge flow separation that occurred at moderate angles of attack might be compared with flow conditions at maximum lift, and methods, such as camber or leading-edge flaps, whereby maximum lift has been improved through an improvement of the flow conditions over the leading edge may be applicable for this case. Either method produces, for a given lift coefficient, a decrease in the angle of the forward part of the airfoil with reference to the direction of the air flow in the immediate vicinity

UNCLASSIFIED

of the leading edge (the upwash); thus, the flow conditions were improved and separation eliminated or delayed to some higher angle of attack or lift coefficient. Accordingly, an investigation was conducted to study the effects of camber corresponding to design-lift coefficients of 0, 0.2, and 0.5 and a 15-percent-chord leading-edge flap on the pressure pulsations of a 6-percent-thick airfoil. Time histories of the instantaneous pressure pulsations acting at eight chordwise stations on the upper surfaces of the airfoils were obtained, and the corresponding flows past the airfoils were recorded by high-speed schlieren motion pictures. The data were obtained at Mach numbers from 0.5 to 1.0 and at corrected angles of attack from  $0^\circ$  to  $8^\circ$ . The leading-edge-flap deflection angle was varied from  $0^\circ$  to  $-15^\circ$ . The Reynolds number of the flow based on the model chord ranged from  $1.2 \times 10^6$  to  $1.7 \times 10^6$ .


#### SYMBOLS

M	free-stream Mach number
q	free-stream dynamic pressure, lb/sq ft
$\Delta p$	double-amplitude pressure pulsation, lb/sq ft
$c_n$	section normal-force coefficient
$\alpha$	angle of attack, deg
$\delta$	leading-edge-flap angle of deflection, deg

#### APPARATUS AND TESTS

Tests were made in the Langley 4- by 19-inch semiopen tunnel (fig. 1). The tunnel conditions, method, and precision of the pressure measurements were identical with those of reference 1.

A photograph of the model installation in the Langley 4- by 19-inch semiopen tunnel is given in figure 2. One of the small electrical induction cells (ref. 2) used in this investigation to obtain time histories of pressure pulsations is shown on a ledge at the bottom center of the photograph. The cells and the recording system possess a relatively flat frequency-response characteristic from 40 to 500 cycles per second. The instrumentation utilizing this type of pressure cell gives a time-history trace of the pressure pulsation on the airfoil surface. The frequencies above 600 cycles per second are highly damped in this installation.



The models tested were 6-percent-thick NACA 64A-series airfoils of 4-inch chord and span; three of the airfoils were cambered for 0, 0.2, and 0.5 design lift coefficients. The other airfoil was a symmetrical NACA 64A006 model having a 15-percent-chord leading-edge flap (fig. 3). The airfoil ordinates are presented in table I. The plain and cambered models had pressure orifices located at 3.1-, 14-, 25-, 37.5-, 50-, 62.5-, 75-, and 87.5-percent-chord stations and the leading-edge-flap model had orifices located at 5.9-, 25-, 37.5-, 50-, 62.5-, 75-, and 87.5-percent-chord stations.

The data were obtained at Mach numbers from 0.5 to approximately 1.0 and at test angles of attack from  $0^\circ$  to  $10^\circ$ . Leading-edge-flap deflections varied from  $0^\circ$  to  $-15^\circ$  from the mean chord line of the model. The pressure-pulsation data were supplemented by high-speed schlieren motion pictures taken at approximately 250 frames per second.

#### REDUCTION OF DATA

The pressure pulsations  $\Delta p$  were selected from oscillograph traces of the instantaneous time history of the pressure at each orifice. A portion of a typical record is shown in figure 4 for an NACA 64A006 airfoil. The pulsation measured from a crest to an adjacent trough of a pressure pulse is the double-amplitude variation of the pressure above and below the average level of the pressure existing at the airfoil orifice. Each gage was referenced to a steady pressure near the average pressure existing locally on the airfoil surface; consequently, these records do not give an indication of the average pressure on the airfoil. Pulsations in the reference pressure were damped out by means of a small-diameter tube, 3 to 5 feet in length, extending from the reference orifice on the end plate to the gage (fig. 3).

The pressure pulsations on the models were characterized by their haphazard occurrence and generally irregular amplitude. Time-history traces of the pressure pulsations for each of the several orifices on the airfoil in general bore a marked resemblance to one another and were approximately in phase (fig. 4). The pressure pulsation selected was of intermediate amplitude and appeared to predominate. The predominant amplitudes  $\Delta p$  that occur frequently throughout the individual traces were considered the typical amplitudes for the particular record. They varied in magnitude from one-half to one-third the value of the maximum-pressure pulses of infrequent occurrence. The pulsating pressures  $\Delta p$  (double amplitude) are expressed in terms of the stream dynamic pressure as  $\frac{\Delta p}{q}$ .

The test angle of attack has been reduced by 20 percent to approximate the incompressible-jet-deflection correction for a semiopen tunnel (ref. 3); the same correction to the angle of attack was used in reference 1. The normal-force coefficients presented for the model with leading-edge flap were determined by an electrical integrator which could not correct for differences in inclination of the normal-force vectors on the flap and on the airfoil. The magnitude of the error introduced has been evaluated from some check computations using the measured pressure distributions and is of the order of 0 to 0.02 in normal-force coefficient.

## RESULTS AND DISCUSSION

Methods of avoiding the early occurrence of the high-speed stall and the associated high-pressure pulsations of thin airfoils have been investigated. An airfoil utilizing camber presented a possible solution to the problem of obtaining improved flow conditions over the forward part of thin airfoils at moderate angles of attack. By appropriate variations of the mean line, the forward part of the airfoil can be more closely aligned with the air stream than is possible for a plain airfoil at a comparable normal-force coefficient. The effect of camber, expressed as design lift coefficients of 0, 0.2, and 0.5, on the variation of chordwise pressure pulsations with angle of attack and Mach number is presented in figures 5, 6, and 7. The basic data contained in these plots show the growth and decay of the pulsating pressures with increasing Mach number and the forward movement of peak pulsations with increase in angle of attack. These variations are generally similar to those observed on the airfoils presented in reference 1.

A direct comparison in figure 8 of the pressure-pulsation data for the plain NACA 64A006 airfoil (fig. 5) with the data for the NACA 65A006 airfoil of reference 1 indicates that the more rearward location of the position of maximum thickness on the latter airfoil produced a large reduction in the pressure-pulsation levels at all comparable Mach numbers and angles of attack. The more favorable performance of the 65A-series airfoils was not known prior to the present investigation. The 64A-series airfoils were selected for the present investigation because these models and their section aerodynamic characteristics were readily available.

An alternative method of obtaining the effect of camber on the flow at the leading edge was through the use of a leading-edge flap. The basic data for the NACA 64A006 airfoil with a 15-percent-chord leading-edge flap at various flap deflections are presented in figure 9. The chordwise variation of the double-amplitude-pressure pulsations with

angle of attack and Mach number for the leading-edge-flap model is generally similar to that shown for the cambered models in figures 5 to 7.

The pressure-pulsation data at constant angle of attack from figures 5 to 7 and 9 have been cross-plotted with normal-force-coefficient data and are presented in figures 10 to 12 to show the changes in pressure pulsations along the chord as affected by Mach number for each of several constant values of the normal-force coefficient. A comparison of the pressure-pulsation data for the symmetrical airfoil at constant normal-force coefficient (fig. 10) with the data for the cambered models (fig. 11) indicates that the general effect of camber was to reduce the level of the pressure pulsations and to move the location of the peak pulsations rearward. The same general effect was observed for the model with leading-edge flap deflected (fig. 12). The reduction in pressure pulsations over the cambered models and over the model with the leading-edge flap appropriately deflected is attributed to the improved flow conditions near the leading edge of the model and the consequent reduction in flow separation and shock unsteadiness.

The effects of each profile change and Mach number on the chord-wise pressure pulsations on NACA 64A-series airfoil sections are summarized in figure 13 at constant normal-force coefficients of 0.4, 0.6, and 0.75. The effect of leakage through the 0.002-inch opening at the flap hinge can be assessed from a comparison of the data for the plain model with the data for flapped model with flap undeflected. Leakage through the flap hinge generally produced somewhat higher peak-pressure pulsations for the lower normal-force coefficients than were observed on the plain model. At the highest value of  $c_n$ , at Mach numbers between 0.5 and 0.8, the pressure pulsations were large for both models.

At a  $c_n$  of 0.4 (fig. 13(a)), pressure pulsations of low amplitude occur on the nose of the symmetrical model at all Mach numbers. Farther rearward on the airfoil at the 40-percent-chord station, a pressure pulsation of large amplitude occurs at a Mach number of 0.8. This large pulsation was alleviated by using an airfoil cambered for a design-lift coefficient of 0.2, or by using a leading-edge-flap deflection of  $-10^\circ$ . The improvement obtained by using an airfoil with a design lift coefficient of 0.5 was larger than that shown for the  $-10^\circ$  flap deflection at all Mach numbers. The leading-edge flap is inferior to the cambered airfoil carrying this load.

At a design normal-force coefficient of 0.6 (fig. 13(b)), the pressure pulsations begin to rise over the forward part of the symmetrical airfoil. The generally favorable effect of either camber or proper flap deflection on the nose-pressure pulsation is shown not only at lower but also at higher Mach numbers. Although camber is not an independent

variable during flight, the flap deflection, however, can be adjusted to obtain the minimum pulsation for various flight conditions.

At a normal-force coefficient of 0.75 (fig. 13(c)), the symmetrical model appears to be operating in a stalled condition with characteristic high-pressure pulsations occurring over the nose at Mach numbers between 0.5 and 0.7. Flow attachment at the nose occurs near a Mach number of 0.8 and the peak-pressure pulsations move rearward. A very large reduction in the magnitude of the pressure pulsation is obtained at this normal-force coefficient by a small amount of camber. Higher camber is even more effective in reducing the pressure pulsations at all Mach numbers except those around 0.8. Similarly, flap deflections of from  $-5^\circ$  to  $-10^\circ$  produced a reduction in the pressure-pulsation level that compares favorably with the reduction obtained by using an airfoil with a design lift coefficient of 0.2.

Investigations (for instance, ref. 4) have shown an adverse shift in the angle of zero lift and a consequent loss of lift for highly cambered models which can aggravate the stability problem in the high subsonic Mach number range. The considerable reduction in the pressure pulsations achieved over a wide Mach number and lift-coefficient range by using either camber or a leading-edge flap suggests that a combination of leading-edge flap and, possibly, a small amount of camber may provide greater flexibility in pressure-pulsation control.

The flow conditions that give rise to the changes in pressure pulsations at a Mach number of 0.7 and  $c_n = 0.75$  presented in figure 13(c) are shown in figure 14. The flow photographs made at approximately 4-millisecond intervals and 4-microsecond duration, indicate that the extensively separated flow on the symmetrical model is removed by using either camber or leading-edge-flap deflection. Flow conditions on the flapped model and the model cambered for a design lift coefficient of 0.2 are similar. For this high lift condition and Mach number, the smallest flow disturbances were obtained on the model using a design lift coefficient of 0.5.

#### CONCLUDING REMARKS

An investigation of the pressure pulsations on a 6-percent-thick 64A-series airfoil revealed that the high pulsations associated with leading-edge flow separation on the basic airfoil were significantly

reduced either by the use of camber or by suitable deflection of a 15-percent-chord leading-edge flap. The optimum camber or flap deflection were dependent on Mach number and normal-force coefficient. Comparison of the data for the basic 64A006 section used in these tests with data previously obtained for the 65A006 section revealed significantly lower pressure pulsations for the 65A006 airfoil.

Langley Aeronautical Laboratory,  
National Advisory Committee for Aeronautics,  
Langley Field, Va.

#### REFERENCES

1. Humphreys, Milton D.: Pressure Pulsations on Rigid Airfoils at Transonic Speeds. NACA RM L51112, 1951.
2. Patterson, John L.: A Miniature Electrical Pressure Gage Utilizing a Stretched Flat Diaphragm. NACA TN 2659, 1952.
3. Katzoff, S., Gardner, Clifford S., Diesendruck, Leo, and Eisenstadt, Bertram J.: Linear Theory of Boundary Effects in Open Wind Tunnels With Finite Jet Lengths. NACA Rep. 976, 1950. (Supersedes NACA TN 1826.)
4. Lindsey, W. F., Stevenson, D. B., and Daley, Bernard N.: Aerodynamic Characteristics of 24 NACA 16-Series Airfoils at Mach Numbers Between 0.3 and 0.8. NACA TN 1546, 1948.



TABLE I.- AIRFOIL ORDINATES

8

NACA 64A006 airfoil		NACA 64A206 airfoil				NACA 64A506 airfoil			
Upper and lower surface same		Upper surface		Lower surface		Upper surface		Lower surface	
Station	Ordinate	Station	Ordinate	Station	Ordinate	Station	Ordinate	Station	Ordinate
0	0	0	0	0	0	0	0	0	0
.5	.485	.454	.539	.546	-.427	.388	.613	.612	-.331
.75	.585	.699	.662	.801	-.504	.624	.769	.876	-.373
1.25	.739	1.192	.858	1.308	-.616	1.107	1.027	1.393	-.423
2.50	1.016	2.432	1.225	2.568	-.803	2.333	1.530	2.667	-.474
5	1.399	4.924	1.758	5.076	-1.036	4.812	2.288	5.188	-.484
7.50	1.684	7.421	2.168	7.579	-1.196	7.304	2.889	7.696	-.457
10	1.919	9.921	2.513	10.079	-1.321	9.803	3.400	10.197	-.418
15	2.283	14.924	3.063	15.076	-1.502	14.812	4.227	15.188	-.323
20	2.557	19.931	3.486	20.069	-1.626	19.828	4.877	20.172	-.225
25	2.757	24.940	3.807	25.060	-1.705	24.850	5.382	25.150	-.124
30	2.896	29.950	4.043	30.050	-1.747	29.876	5.764	30.124	-.022
35	2.977	34.961	4.201	35.039	-1.753	34.903	6.035	35.097	.085
40	2.999	39.973	4.278	40.027	-1.720	39.932	6.195	40.068	.199
45	2.945	44.985	4.259	45.015	-1.631	44.962	6.231	45.038	.341
50	2.825	49.997	4.155	50.003	-1.495	49.991	6.151	50.009	.501
55	2.653	55.007	3.979	54.993	-1.327	55.019	5.969	54.981	.663
60	2.438	60.017	3.740	59.983	-1.136	60.043	5.692	59.957	.816
65	2.188	65.026	3.443	64.974	-.933	65.064	5.324	64.936	.950
70	1.907	70.033	3.090	69.967	-.724	70.082	4.862	69.918	1.052
75	1.602	75.039	2.685	74.961	-.519	75.096	4.300	74.904	1.102
80	1.285	80.046	2.219	79.954	-.349	80.115	3.617	79.885	1.057
85	.967	85.045	1.687	84.955	-.245	85.113	2.764	84.887	.844
90	.649	90.032	1.138	89.968	-.158	90.079	1.870	89.921	.582
95	.331	95.016	.576	94.984	-.086	95.040	.942	94.960	.284
100	.013	100	.013	100	-.013	100	.013	100	-.013
L.E. radius: 0.246 T.E. radius: 0.014		L.E. radius: 0.246 T.E. radius: 0.014 Slope of radius through L.E.: 0.095				L.E. radius: 0.246 T.E. radius: 0.014 Slope of radius through L.E.: 0.238			

NACA

NACA RM L52G22

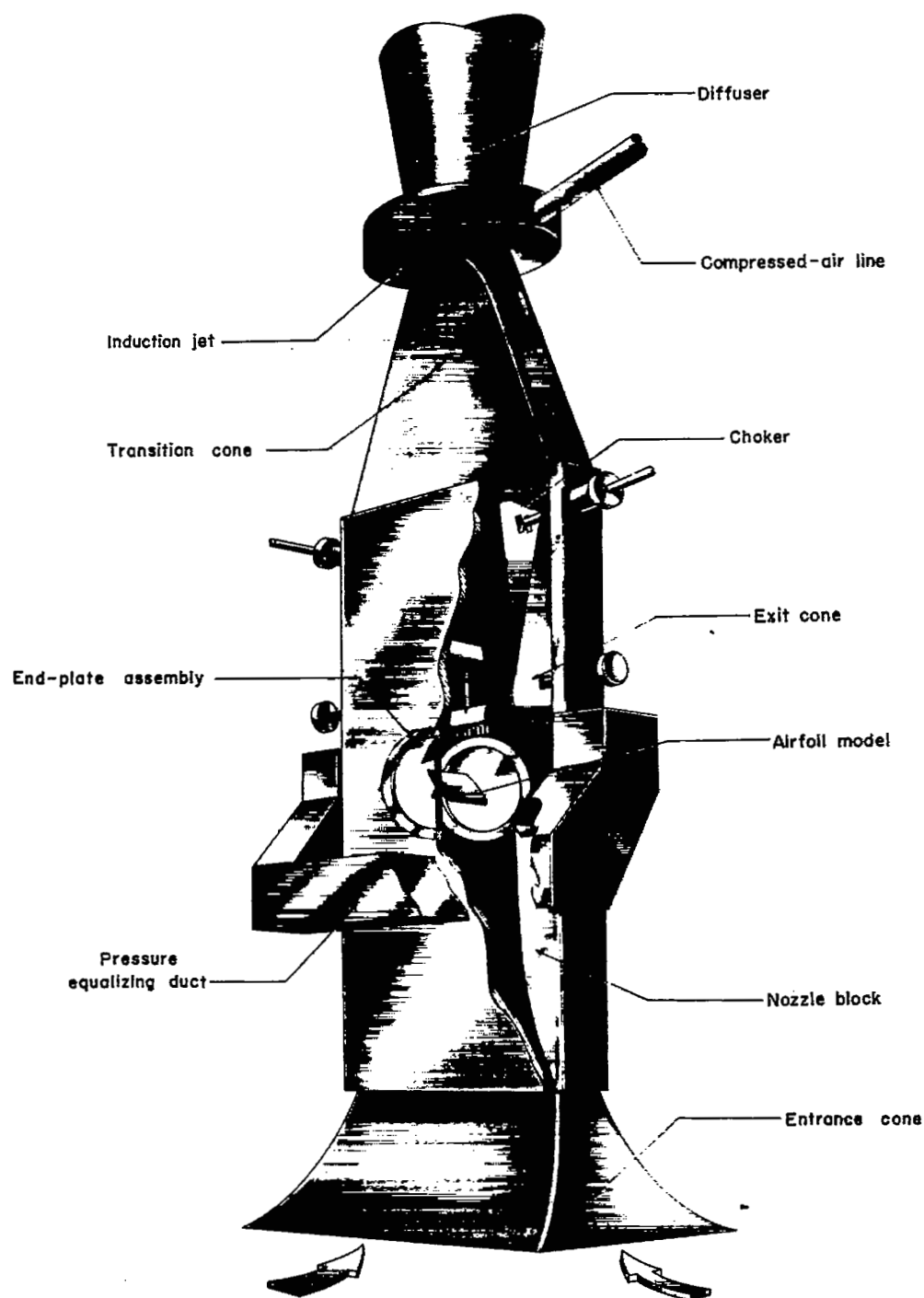


Figure 1.- Langley 4-by 19-inch semiopen tunnel.

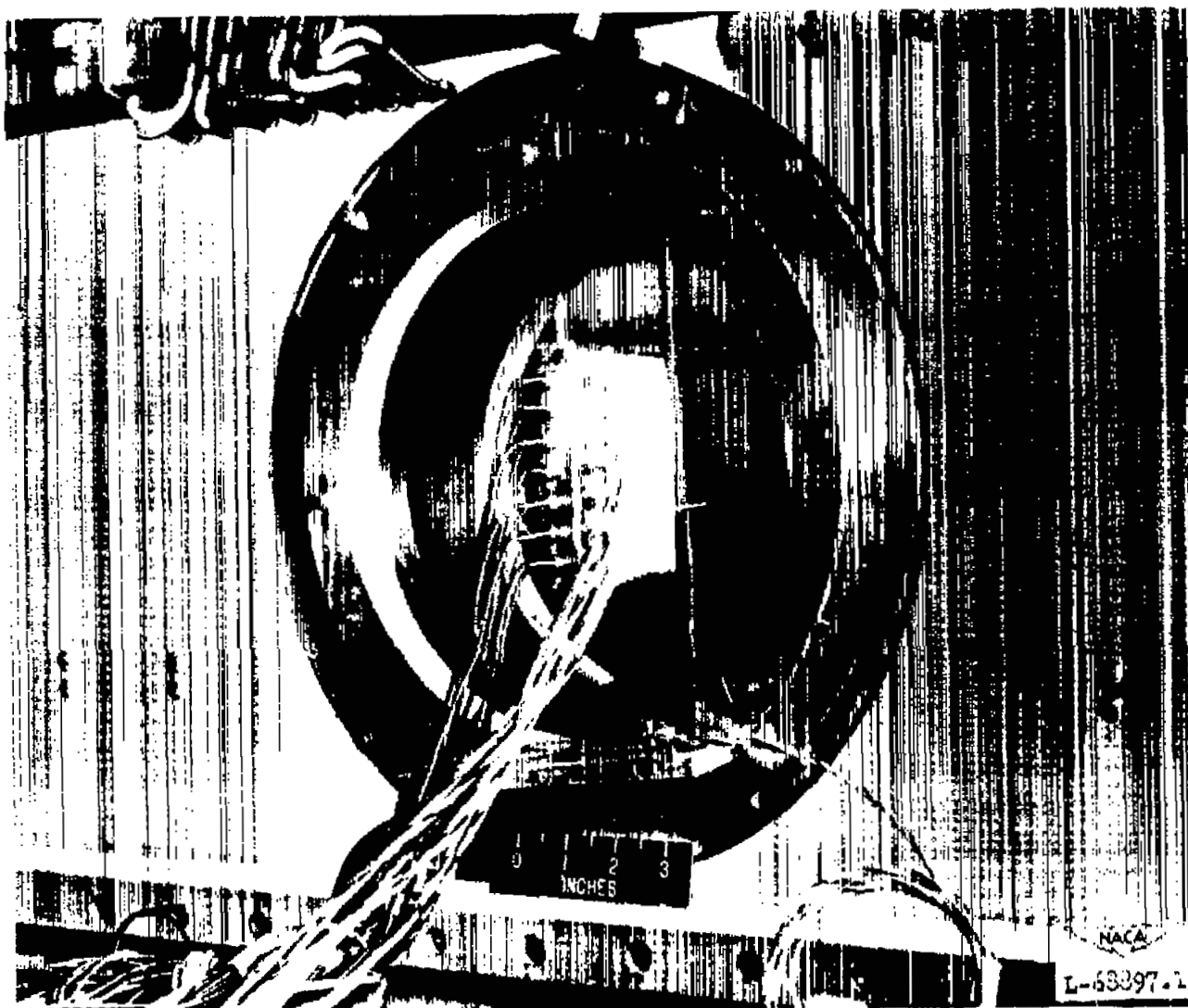


Figure 2.- Model installation in the Langley 4- by 19-inch semiopen tunnel.

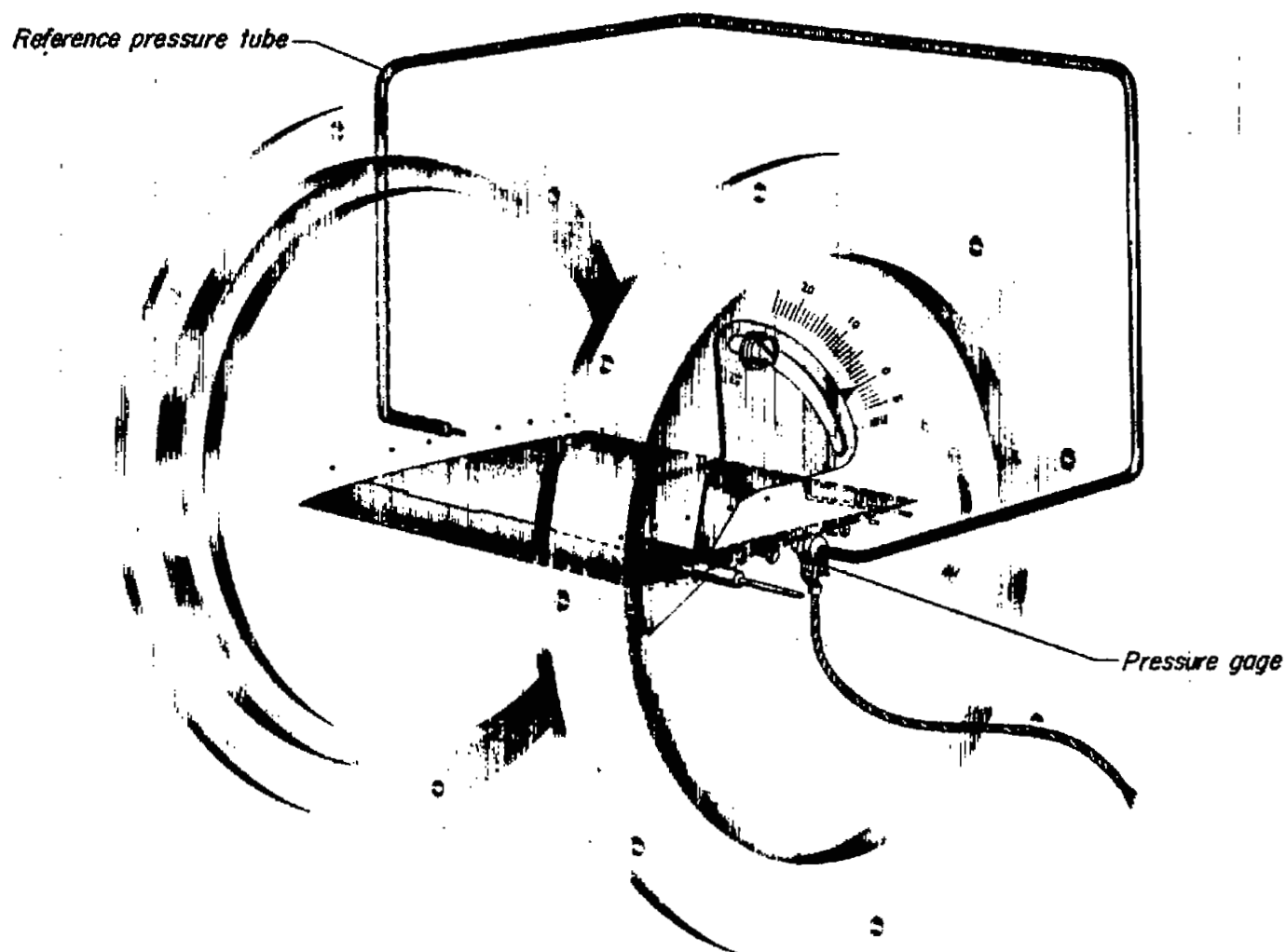


Figure 3.- Installation in end plates of the NACA 64A006 airfoil with 15-percent-chord leading-edge flap.

NACA  
L-75170

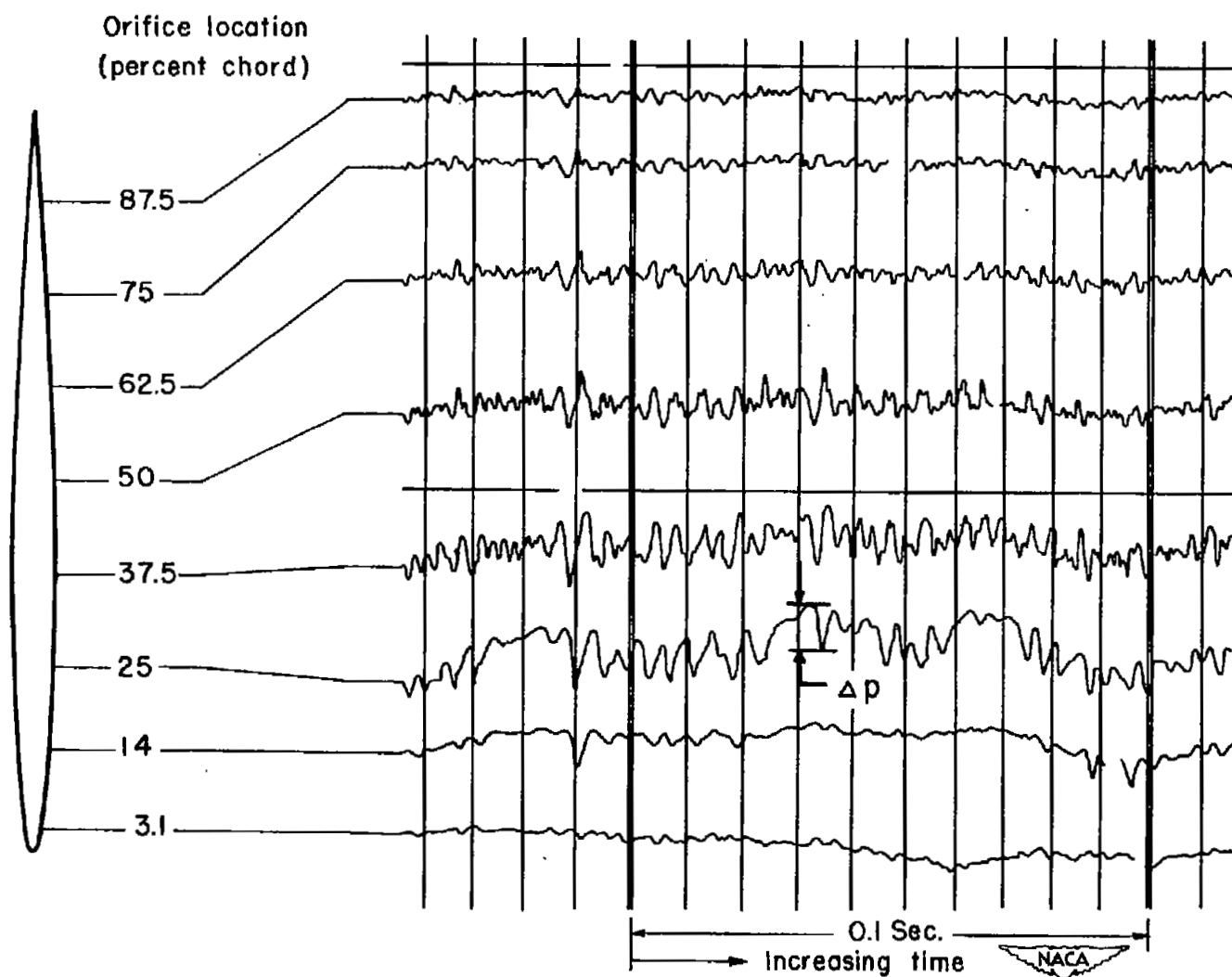


Figure 4.- Airfoil profile and orifice locations with typical records of pulsating pressures on NACA 64A006 airfoil.  $\alpha = 1.6^\circ$ ;  $M = 0.85$ .

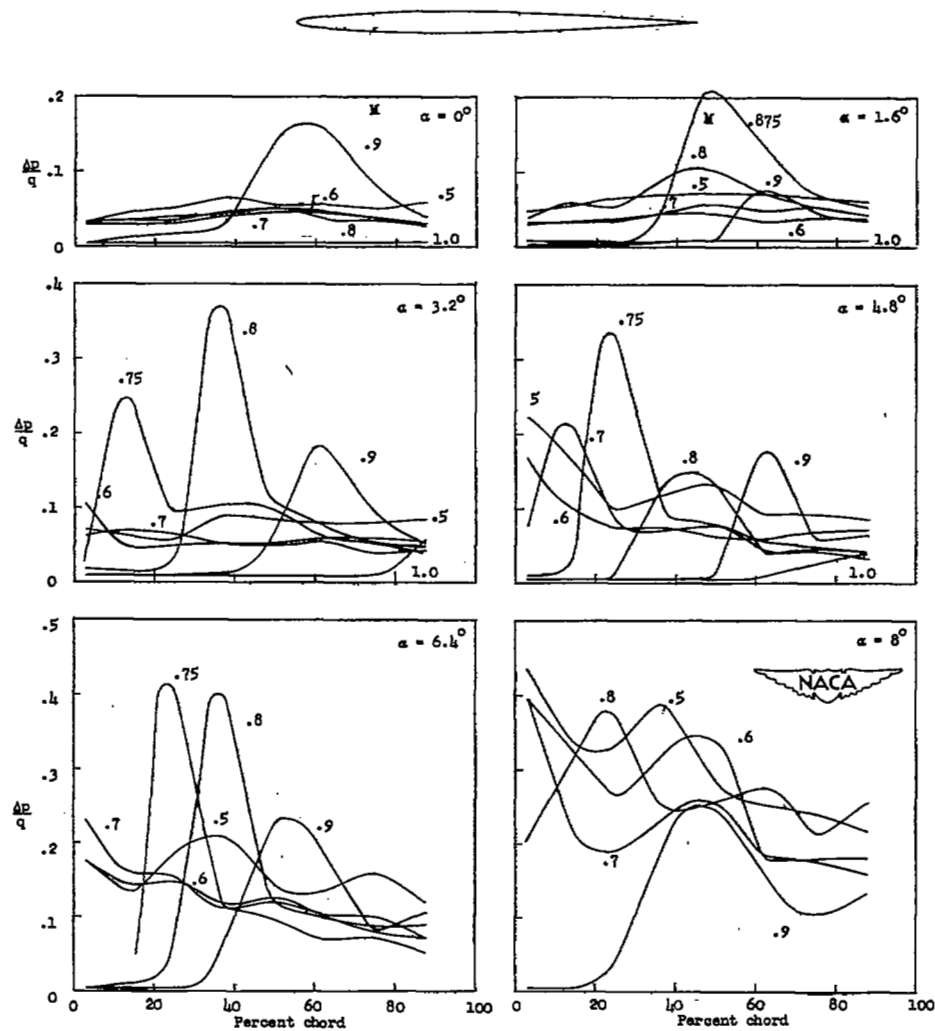


Figure 5.- Chordwise pressure pulsations as affected by Mach number and angle of attack for an NACA 64A006 airfoil.

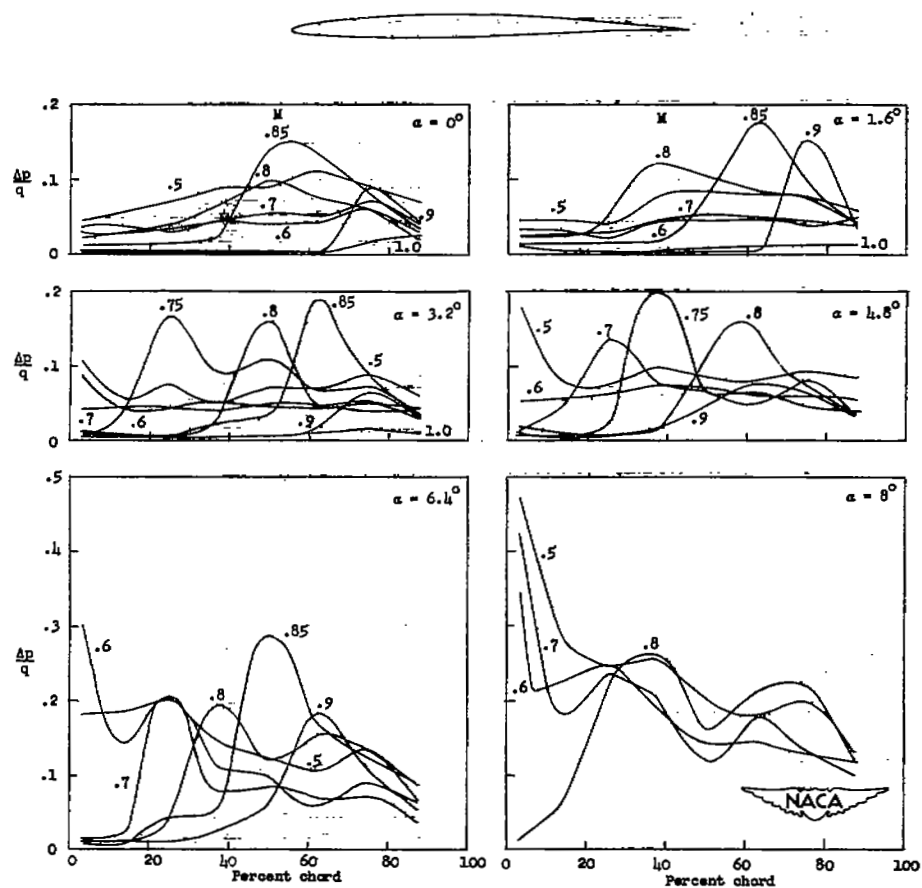


Figure 6.- Chordwise pressure pulsations as affected by Mach number and angle of attack for an NACA 64A206 airfoil.

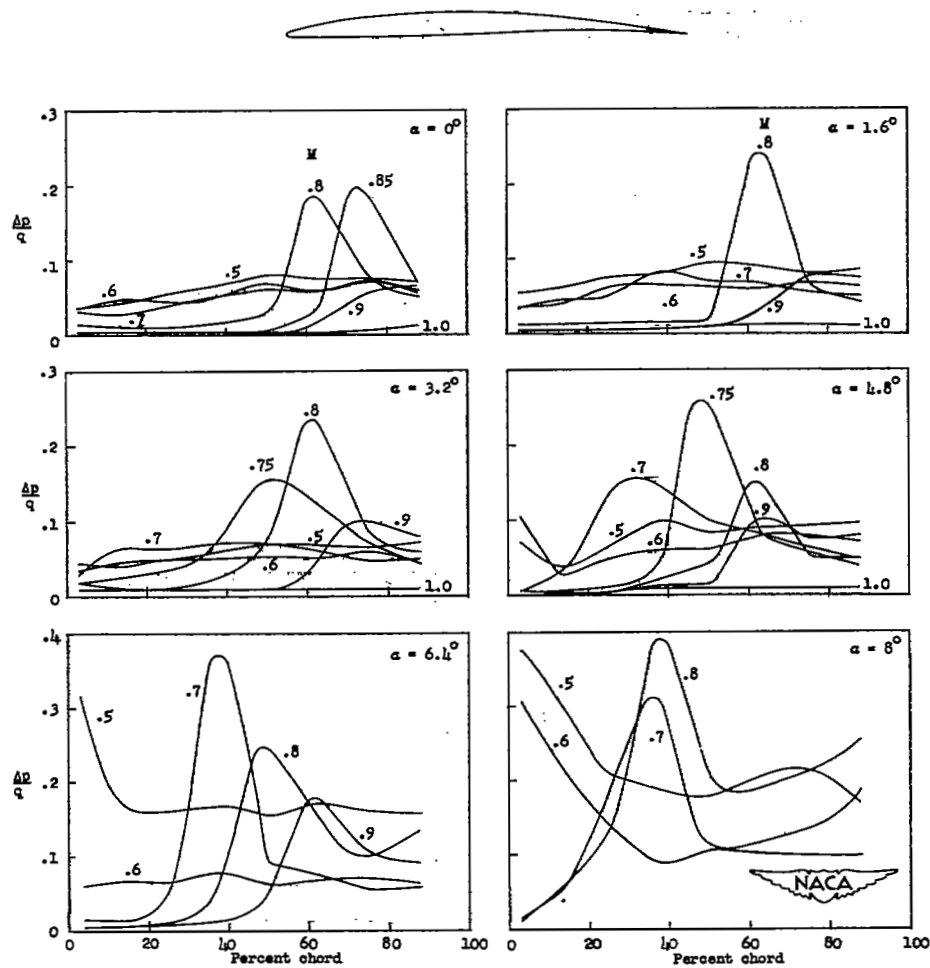


Figure 7.- Chordwise pressure pulsations as affected by Mach number and angle of attack for an NACA 64A506 airfoil.



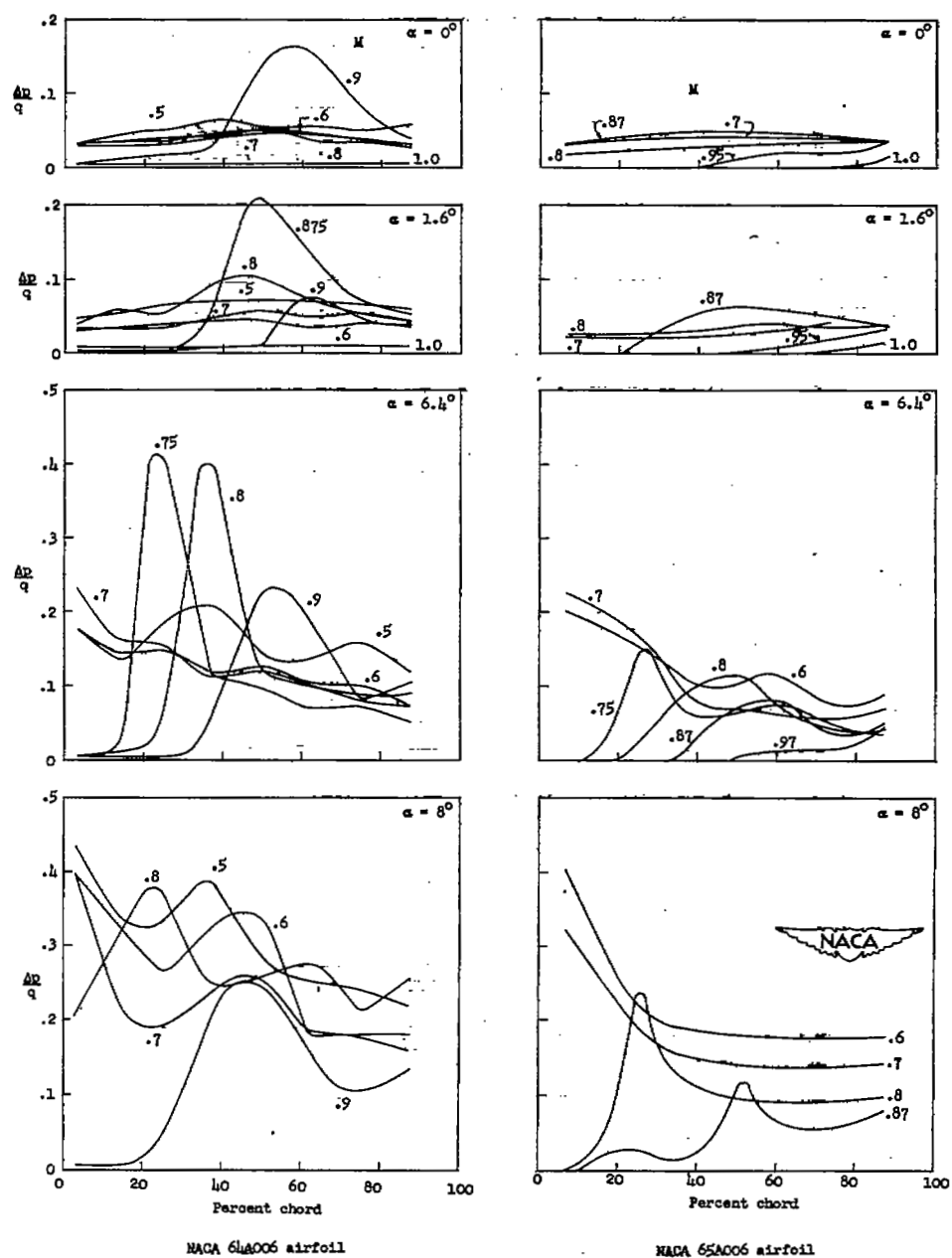
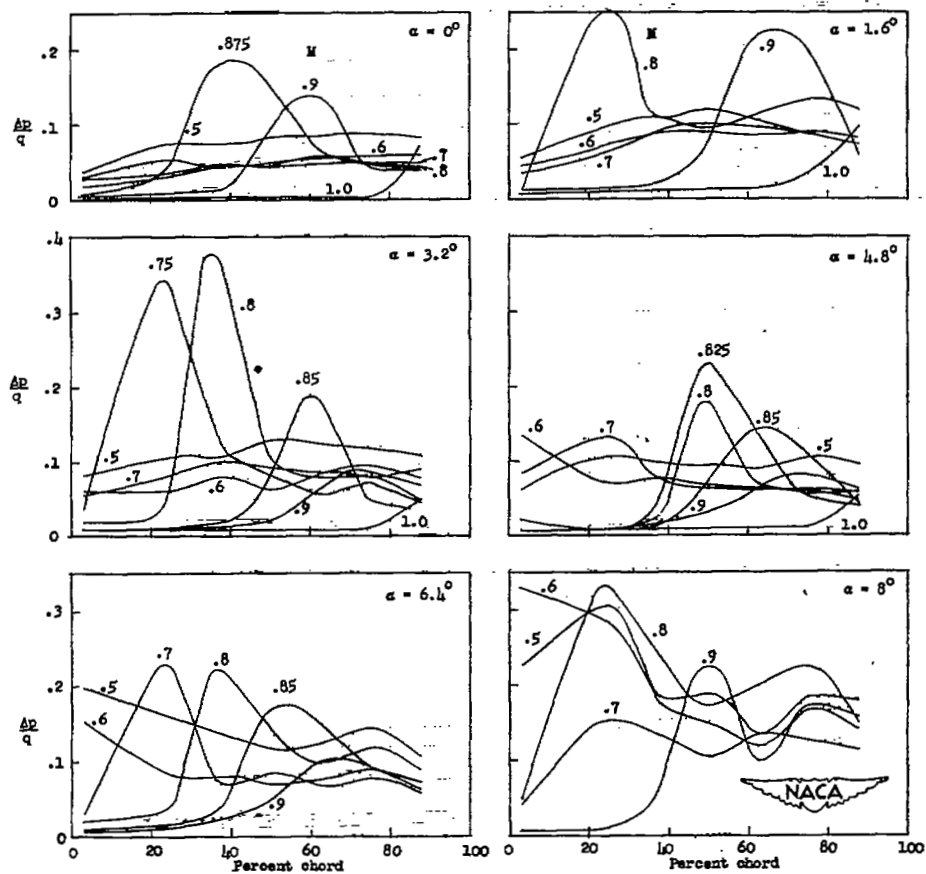


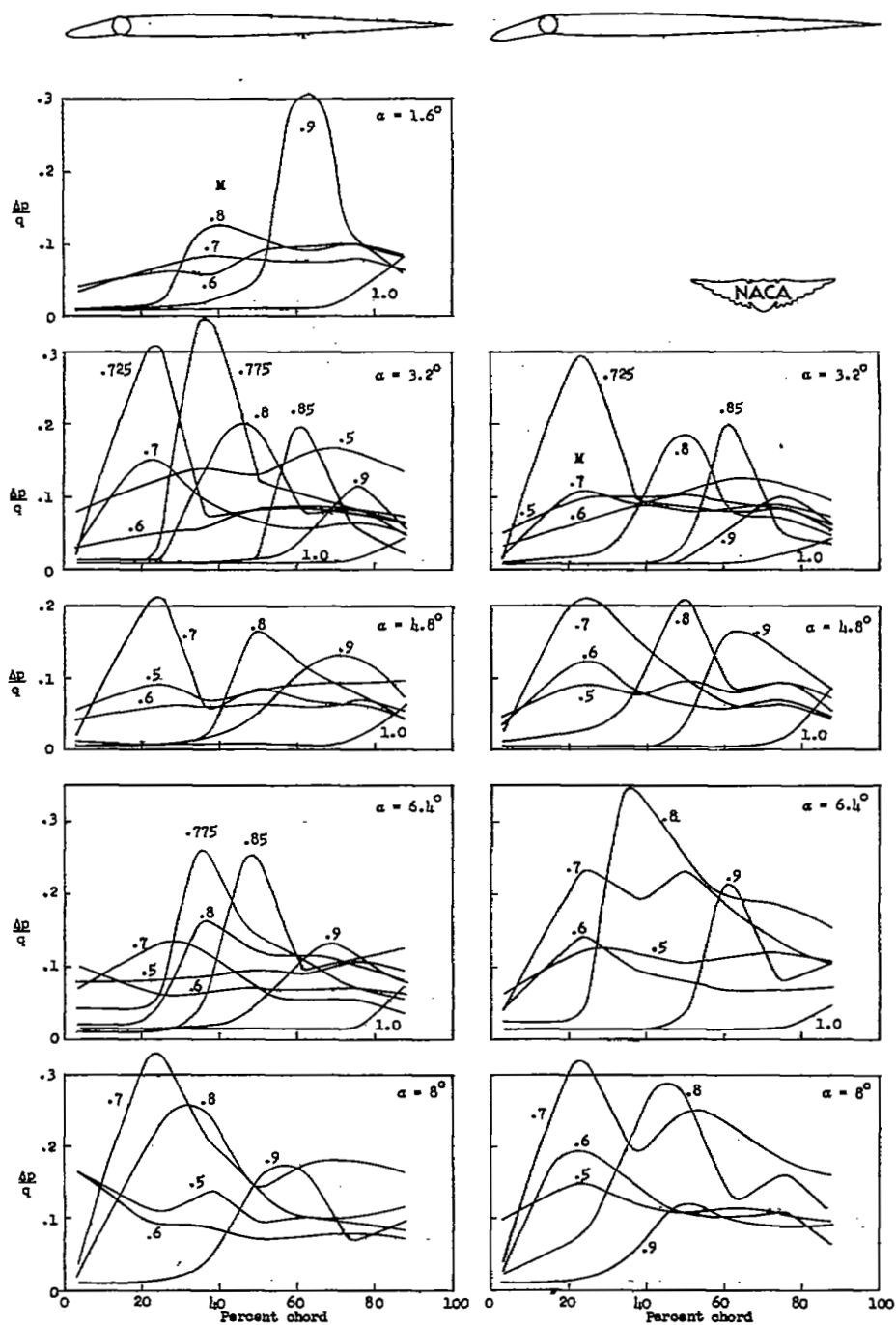
Figure 8.- Comparison of pressure-pulsation data for the NACA 64A006 and NACA 65A006 airfoils.





(b) Leading-edge-flap deflection,  $\delta = -5^\circ$ .

Figure 9.- Continued.



(c) Leading-edge-flap deflection,  
 $\delta = -10^\circ$ .

(d) Leading-edge-flap deflection,  
 $\delta = -15^\circ$ .

Figure 9.- Concluded.

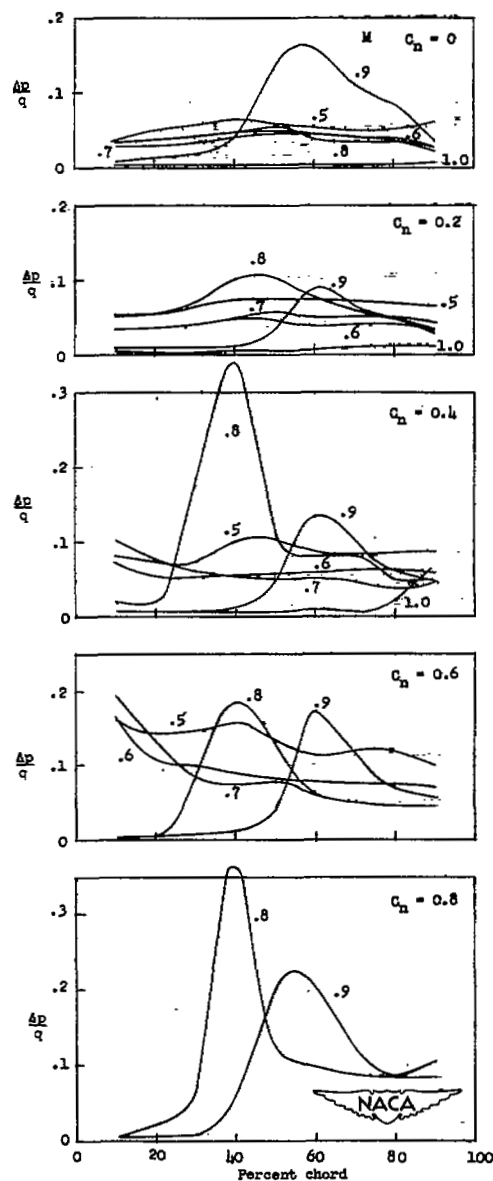
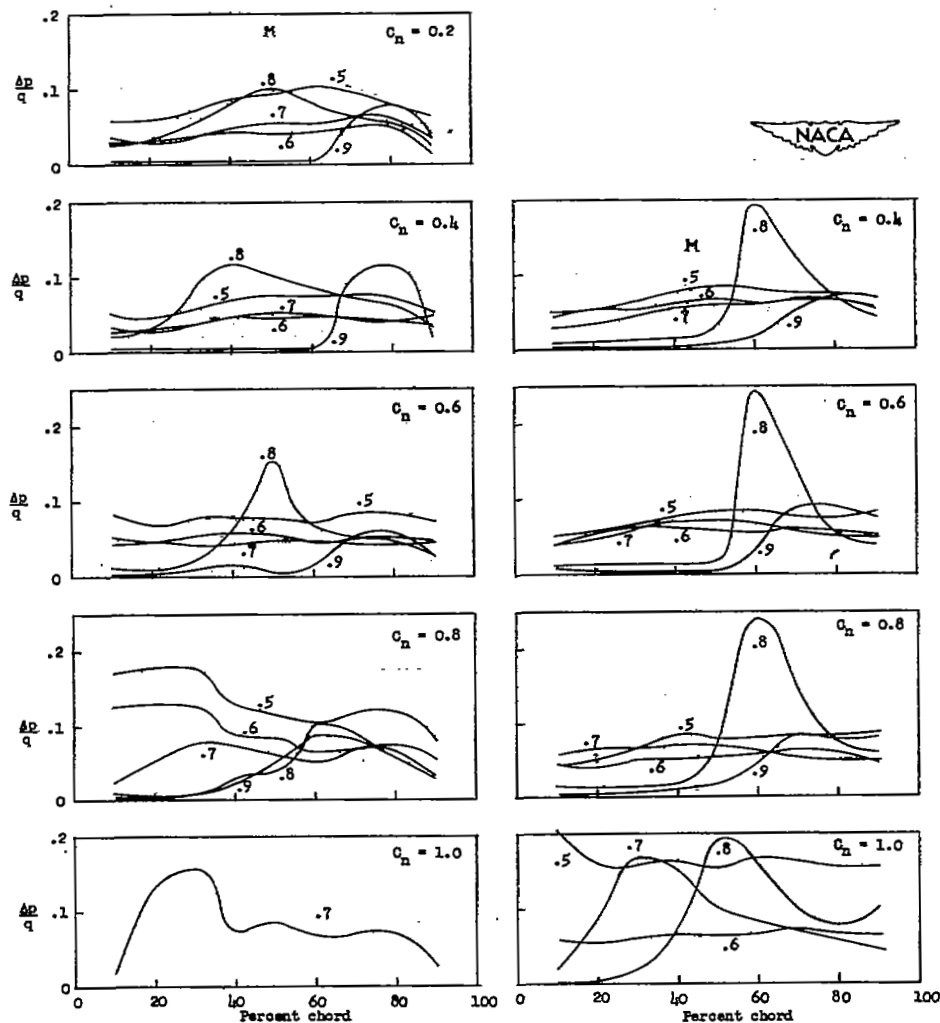


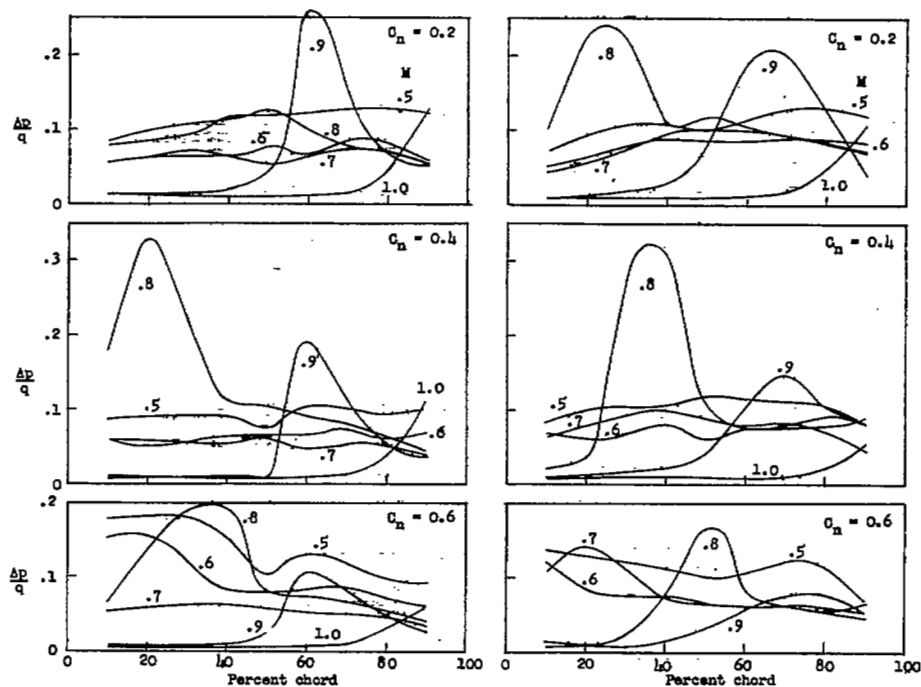
Figure 10.- Chordwise pressure pulsations as affected by Mach number and normal-force coefficient for an NACA 64A006 airfoil.



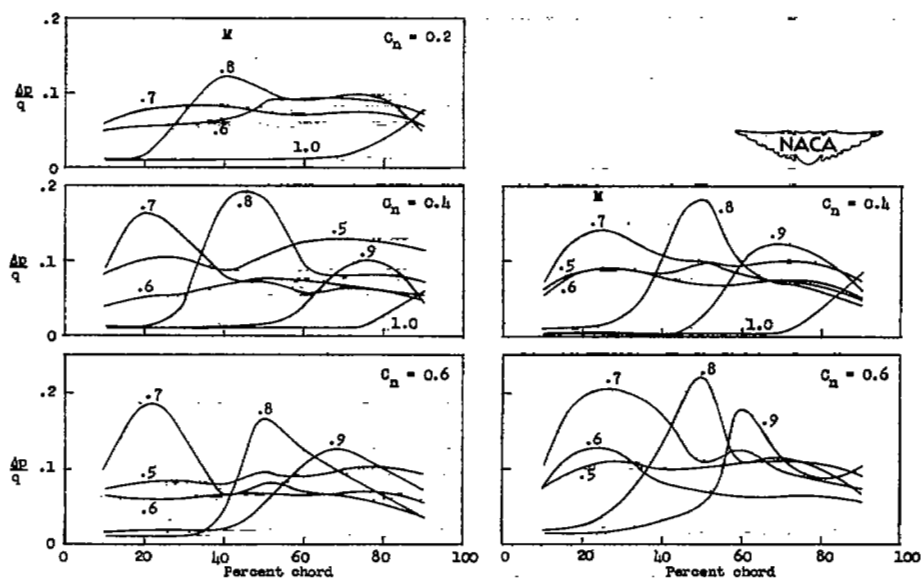
(a) NACA 64A206 airfoil.

(b) NACA 64A506 airfoil.

Figure 11.- Chordwise pressure pulsations as affected by airfoil camber and normal-force coefficient.



(a) Leading-edge-flap deflection,  $\delta = 0^\circ$ . (b) Leading-edge-flap deflection,  $\delta = -5^\circ$ .



(c) Leading-edge-flap deflection,  $\delta = -10^\circ$ . (d) Leading-edge-flap deflection,  $\delta = -15^\circ$ .

Figure 12.- Chordwise pressure pulsations as affected by Mach number and normal-force coefficient for an NACA 64A006 airfoil with leading-edge flap.

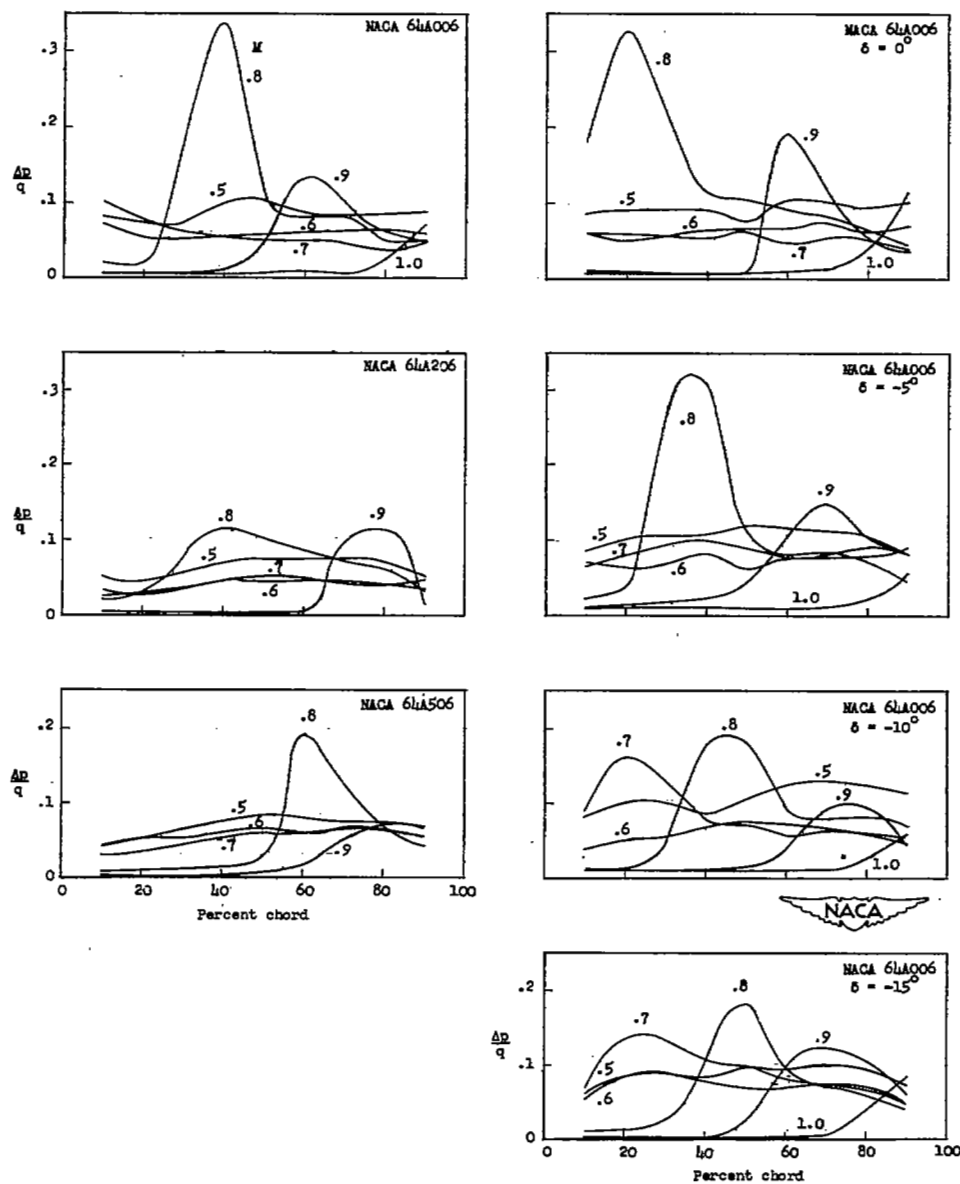
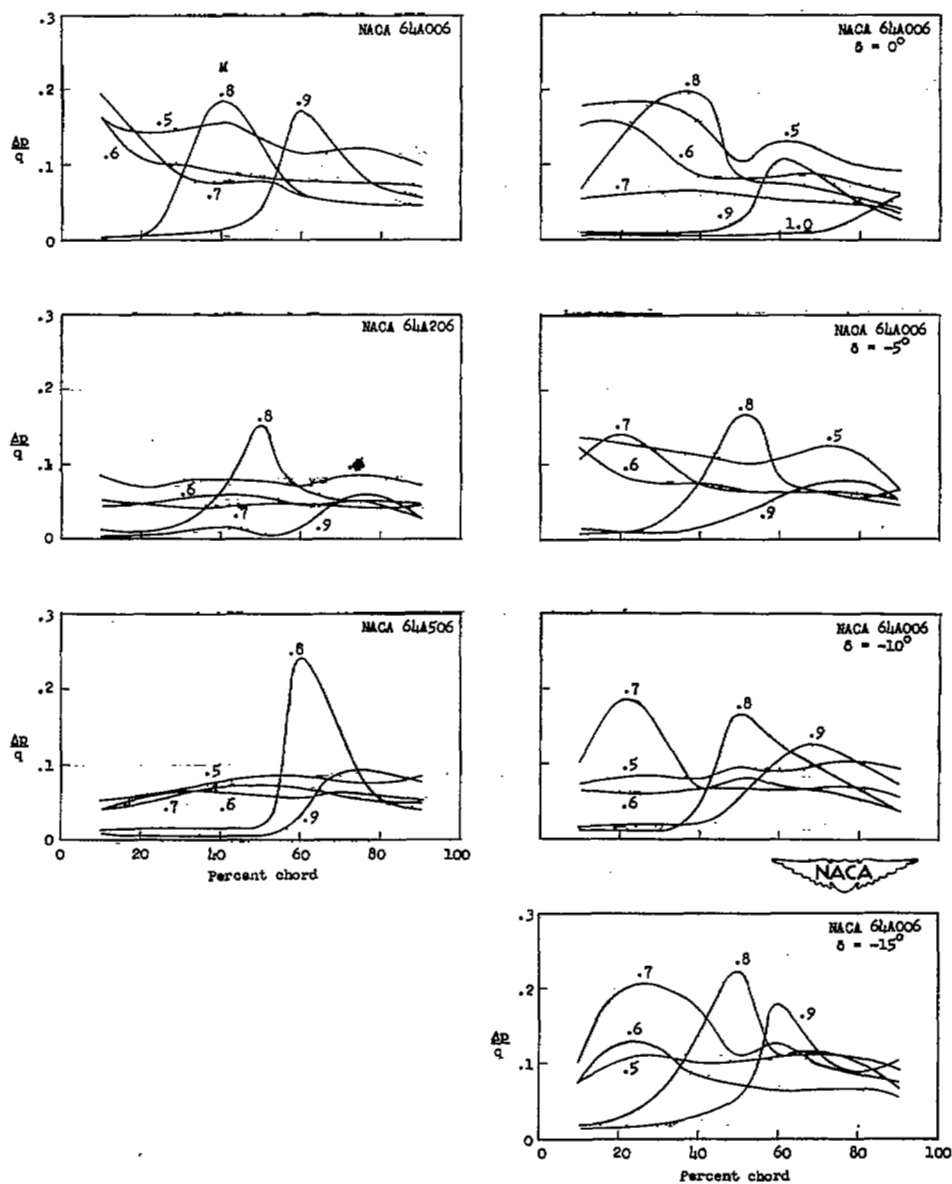
(a)  $c_n = 0.4$ .

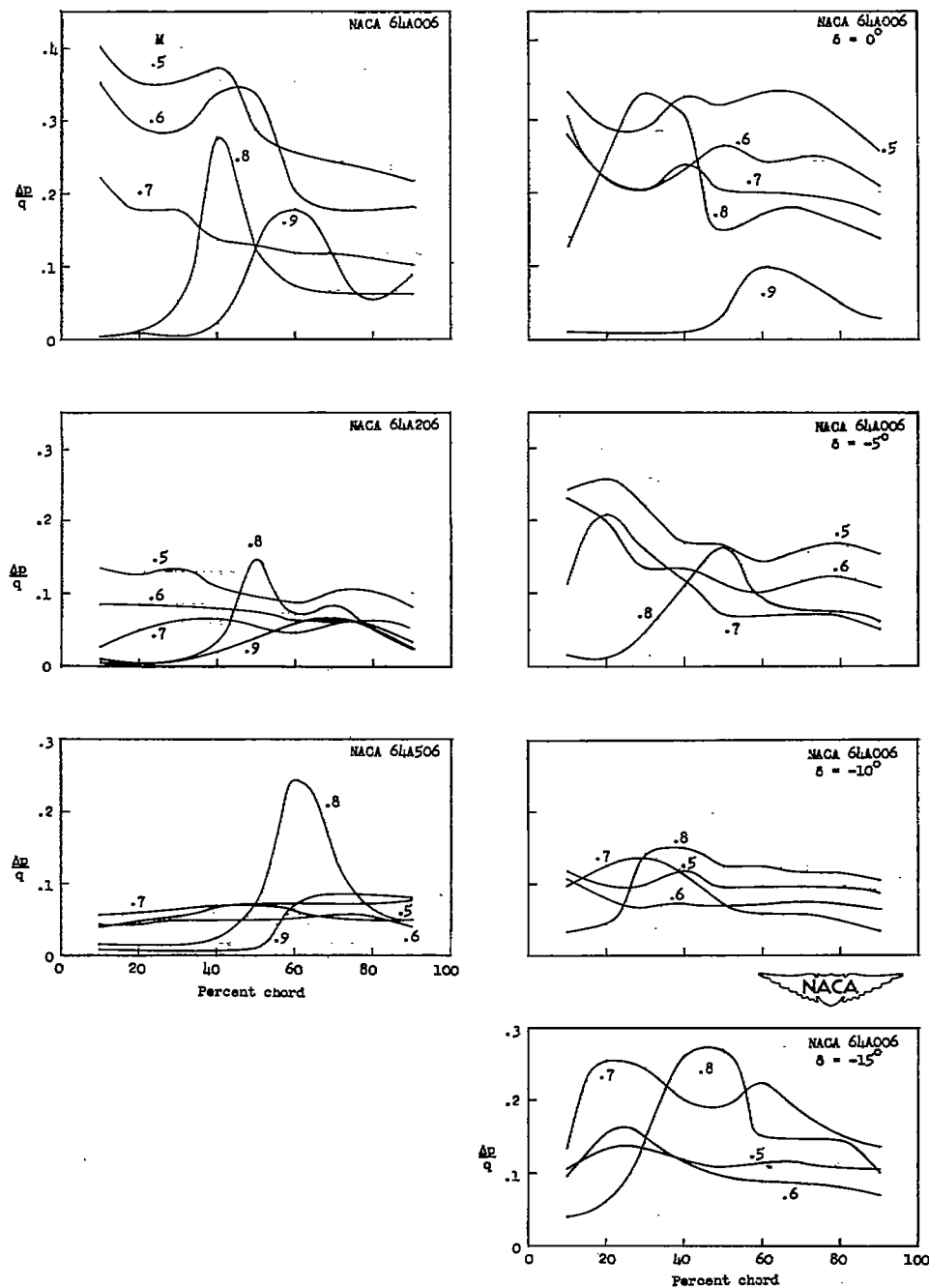
Figure 13.- The effect of camber, leading-edge-flap deflection, and Mach number on the chordwise pressure pulsations on the NACA 64A-series airfoil section at constant  $c_n$  values.





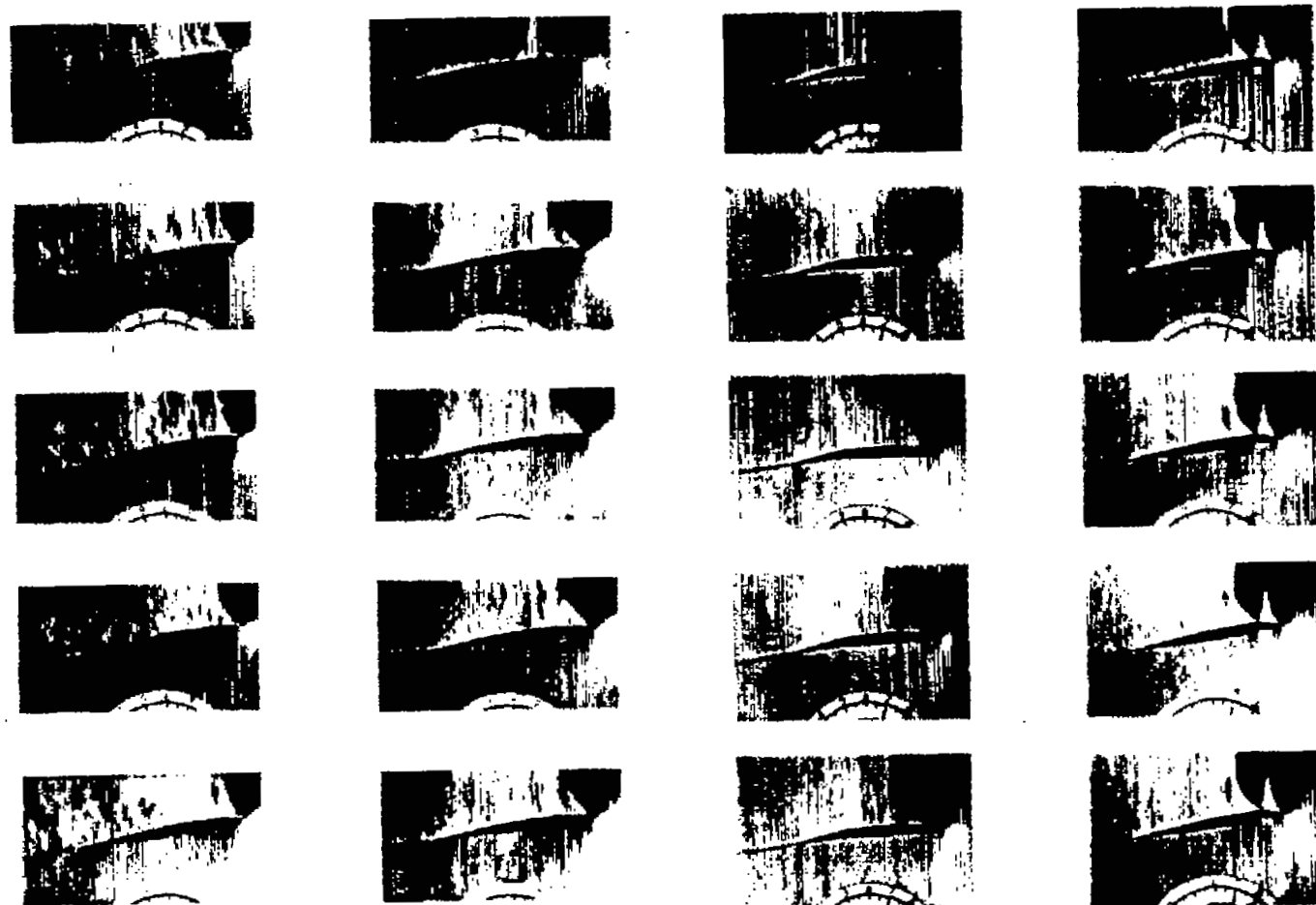
(b)  $c_n = 0.6$ .

Figure 13.- Continued.



(c)  $c_n = 0.75$ .

Figure 13.- Concluded.



NACA 64A006

NACA 64A206

NACA 64A506

NACA 64A006  
 $\delta = -10^\circ$ 

Figure 14.- Effect of camber and leading-edge-flap deflection on flow about 6-percent-thick airfoil.  $M = 0.7$ ;  $c_n \approx 0.75$ .

NACA  
L-75171

# SECURITY INFORMATION

NASA Technical Library



3 1176 01436 9376

